

Heat transport by Dirac fermions in normal/superconducting graphene junctions

Takehito Yokoyama¹, Jacob Linder² and Asle Sudbø²

¹ Department of Applied Physics, Nagoya University, Nagoya, 464-8603, Japan

² Department of Physics, Norwegian University of Science and Technology, N-7491 Trondheim, Norway

(Dated: October 29, 2018)

We study heat transport in normal/superconducting graphene junctions. We find that while the thermal conductance displays the usual exponential dependence on temperature, reflecting the s -wave symmetry of the superconductor, it exhibits an unusual oscillatory dependence on the potential height or the length of the barrier region. This oscillatory dependence stems from the emergent low-energy relativistic nature of fermions in graphene, essentially different from the result in conventional normal metal/superconductor junctions.

The recent progress in practical fabrication techniques for a monoatomic layer of graphite, called graphene, has allowed for experimental studies of this system, which in turn has triggered a tremendous interest^{1,2,3,4,5,6,7}. Graphene is a two-dimensional system of carbon atoms, and the low-energy electrons in graphene are governed by Dirac equation. Up to now, intensive studies on graphene have been conducted for instance quantum Hall effect^{6,8,9}, minimum conductivity⁷ and bipolar supercurrent¹⁰.

From applied physics point of view, graphene is also an important material. Graphene exhibits high mobility and carrier density controllable by gate voltage, which makes it well suited for achieving device applications.^{5,6,11,12} In order to apply graphene to electric devices, it is an important issue to clarify characteristics of transport phenomena in graphene.

In conventional normal metal/superconductor junctions, it is known that electric and thermal conductances reflect the magnitude or symmetry of the gap of the superconductor.^{13,14} While conductance in normal/superconductor graphene junction has been studied,^{15,16,17} thermal conductance in the same junction has not yet been investigated. The study of the thermal conductance in normal/superconductor graphene junction will complement the study of the conductance in the same junction.

In this paper, we study heat transport in normal/superconducting graphene junctions. We find that the thermal conductance has an exponential dependence on temperature, which reflects the s -wave symmetry of the superconductor. However, it displays an oscillatory dependence on the potential height or the length of the barrier region. This oscillatory dependence stems from the relativistic nature of fermions in graphene, and differs in an essential way from the result in the conventional normal metal/superconductor junctions.

We briefly present the formalism to be used in this paper, following Ref.¹⁷. Consider a two dimensional normal/insulating/superconducting graphene junction¹⁸ where the superconducting (normal) region is located in the semi-infinite regions $x > L$ ($x < 0$). The proposed experimental setup of our model is shown in Fig. 1. By exploiting the valley degeneracy,¹⁹ the Bogoliubov-de Gennes equation for the junction in the xy -plane reads

$$\begin{pmatrix} H - E_F \hat{1} & \Delta \hat{1} \\ \Delta^\dagger \hat{1} & E_F \hat{1} - H \end{pmatrix} \begin{pmatrix} u \\ v \end{pmatrix} = E \begin{pmatrix} u \\ v \end{pmatrix} \quad (1)$$

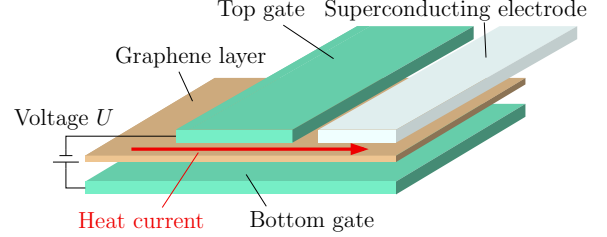


FIG. 1: (color online) The proposed experimental setup to measure heat transport by Dirac fermions in a graphene normal/superconductor proximity structure. The top and bottom gate allow for the chemical potential in the middle region to be adjusted.

with $H = v_F(k_x \sigma_x + k_y \sigma_y)$. The superconducting order parameter reads

$$\Delta = \Delta(T) e^{i\phi} \Theta(x - L), \quad (2)$$

where $\Theta(x)$ is the Heaviside step function, while ϕ is the phase corresponding to the globally broken $U(1)$ symmetry in the superconductor. Also, $v_F \approx 10^6$ m/s is the energy-independent Fermi velocity for graphene, σ_i ($i = x, y$) denotes the Pauli matrices, E is the excitation energy, and u and v denote the electron-like and hole-like excitations, respectively, described by the wave-function. The Pauli matrices operate on the two triangular sublattice space of the honeycomb structure, corresponding to the A and B atoms. The linear dispersion relation is a reasonable approximation even for Fermi levels as high as 1 eV,²⁰ such that the fermions in graphene behave like massless Dirac fermions in the low-energy regime.

Let us consider an incident electron from the normal side of the junction ($x < 0$) with energy E . For positive excitation energies $E > 0$, the eigenvectors and corresponding momentum of the particles read

$$\psi_+^e = [1, e^{i\theta}, 0, 0]^T e^{ip^e \cos \theta x}, \quad p^e = (E + E_F)/v_F, \quad (3)$$

for a right-moving electron at angle of incidence θ , while a left-moving electron is described by the substitution $\theta \rightarrow \pi - \theta$. The superscript T denotes the transpose. If Andreev-reflection takes place, a left-moving hole with energy E and angle of reflection θ_A is generated with corresponding wavefunction

$$\psi_-^h = [0, 0, 1, e^{-i\theta_A}]^T e^{-ip^h \cos \theta_A x}, \quad p^h = (E - E_F)/v_F, \quad (4)$$

where the superscript e (h) denotes an electron-like (hole-like) excitation. Since translational invariance in the y -direction holds, the corresponding component of momentum is conserved. This condition allows for determination of the Andreev-reflection angle θ_A via $p^h \sin \theta_A = p^e \sin \theta$. From this equation, one infers that there is no Andreev-reflection ($\theta_A = \pm\pi/2$) for angles of incidence above the critical angle

$$\theta_c = \sin^{-1}(|E - E_F|/(E + E_F)). \quad (5)$$

On the superconducting side of the system ($x > L$), the possible wavefunctions for transmission of a right-moving quasiparticle with a given excitation energy $E > 0$ reads

$$\begin{aligned} \Psi_+^e &= \left(u, ue^{i\theta^+}, ve^{-i\phi}, ve^{i(\theta^+-\phi)} \right)^T \\ &\times e^{iq^e \cos \theta^+ x}, \quad q^e = (E'_F + \sqrt{E^2 - \Delta^2})/v_F, \end{aligned} \quad (6)$$

$$\begin{aligned} \Psi_-^h &= \left(v, ve^{i\theta^-}, ue^{-i\phi}, ue^{i(\theta^--\phi)} \right)^T \\ &\times e^{iq^h \cos \theta^- x}, \quad q^h = (E'_F - \sqrt{E^2 - \Delta^2})/v_F. \end{aligned} \quad (7)$$

The coherence factors are given by²¹

$$u = \sqrt{\frac{1}{2} \left(1 + \frac{\sqrt{E^2 - \Delta^2}}{E} \right)}, \quad (8)$$

$$v = \sqrt{\frac{1}{2} \left(1 - \frac{\sqrt{E^2 - \Delta^2}}{E} \right)}. \quad (9)$$

Above, we have defined $\theta^+ = \theta_S^e$ and $\theta^- = \pi - \theta_S^h$. The transmission angles $\theta_S^{(i)}$ for the electron-like and hole-like quasiparticles are given by $q^{(i)} \sin \theta_S^{(i)} = p^e \sin \theta$, $i=e,h$. Note that in all the wavefunctions listed above, for clarity we have not included a common phase factor $e^{ik_y y}$ which corresponds to the conserved momentum in the y -direction.

It is appropriate to insert the restriction which will be used throughout the paper, namely $\Delta \ll E'_F$. Since we are using a mean-field approach to describe the superconducting part of the Hamiltonian, phase-fluctuations of the order parameter have to be small²².

We define the wavefunctions in the normal, insulating and superconducting regions by ψ , $\tilde{\psi}_I$ and Ψ , respectively, with

$$\psi = \psi_+^e + r\psi_-^e + r_A\psi_-^h, \quad (10)$$

$$\tilde{\psi}_I = \tilde{t}_1\tilde{\psi}_+^e + \tilde{t}_2\tilde{\psi}_-^e + \tilde{t}_3\tilde{\psi}_+^h + \tilde{t}_4\tilde{\psi}_-^h, \quad (11)$$

$$\Psi = t^e\Psi_+^e + t^h\Psi_-^h. \quad (12)$$

The wavefunctions $\tilde{\psi}$ differ from ψ in that the Fermi energy is shifted by an external potential, such that $E_F \rightarrow E_F - U$ where U is the barrier height. Also, note that the trajectories of the quasiparticles in the insulating region, defined by the angles θ and $\tilde{\theta}_A$, differ by the same substitution:

$$\sin \tilde{\theta} / \sin \theta = (E + E_F)/(E + E_F - U), \quad (13)$$

$$\sin \tilde{\theta}_A / \sin \theta = (E + E_F)/(E - E_F + U). \quad (14)$$

Note that the subscript \pm on the wavefunctions indicates the direction of momentum, which is in general different from the group velocity direction.

By matching the wavefunctions at both interfaces, $\psi|_{x=0} = \tilde{\psi}_I|_{x=0}$ and $\tilde{\psi}_I|_{x=L} = \Psi|_{x=L}$,²³ we obtain the following expressions for the normal reflection coefficient r and the Andreev-reflection coefficient r_A :¹⁷

$$r = t_e(A + C) + t_h(B + D) - 1, \quad (15)$$

$$r_A = t_e(A' + C') + t_h(B' + D'), \quad (16)$$

where the transmission coefficients read

$$t_e = 2 \cos \theta [e^{-i\theta_A}(B' + D') - (B'e^{-i\tilde{\theta}_A} - D'e^{i\tilde{\theta}_A})] \rho^{-1}, \quad (17)$$

$$t_h = t_e [e^{i\theta_A}(A'e^{-i\tilde{\theta}_A} - C'e^{i\tilde{\theta}_A}) - A' - C'] [B' + D' - e^{i\theta_A}(B'e^{-i\tilde{\theta}_A} - D'e^{i\tilde{\theta}_A})]^{-1}, \quad (18)$$

$$\begin{aligned} \rho &= [e^{-i\theta_A}(B' + D') - (B'e^{-i\tilde{\theta}_A} - D'e^{i\tilde{\theta}_A})] [e^{-i\theta}(A + C) + (Ae^{i\tilde{\theta}} - Ce^{-i\tilde{\theta}})] \\ &- [(De^{-i\tilde{\theta}} - Be^{i\tilde{\theta}}) - e^{-i\theta}(B + D)] [A'e^{-i\tilde{\theta}_A} - C'e^{i\tilde{\theta}_A} - e^{-i\theta_A}(A' + C')] \end{aligned} \quad (19)$$

and we have introduced the auxiliary quantities

$$\begin{aligned} A &= ue^{i(q^+-p^+)} [1 - (e^{i\tilde{\theta}} - e^{i\theta^+})(2 \cos \tilde{\theta})^{-1}], \\ B &= ve^{i(q^- - p^+)} [1 - (e^{i\tilde{\theta}} - e^{i\theta^-})(2 \cos \tilde{\theta})^{-1}], \\ C &= ue^{i(p^+ + q^+)} (e^{i\tilde{\theta}} - e^{i\theta^+})(2 \cos \tilde{\theta})^{-1}, \\ D &= ve^{i(p^+ + q^-)} (e^{i\tilde{\theta}} - e^{i\theta^-})(2 \cos \tilde{\theta})^{-1}, \end{aligned} \quad (20)$$

$$\begin{aligned} A' &= ve^{i(q^+ + p^- - \phi)} [1 + (e^{i\theta^+} - e^{-i\tilde{\theta}_A})(2 \cos \tilde{\theta}_A)^{-1}], \\ B' &= ue^{i(q^- + p^- - \phi)} [1 + (e^{i\theta^-} - e^{-i\tilde{\theta}_A})(2 \cos \tilde{\theta}_A)^{-1}], \\ C' &= ve^{i(q^+ - p^- - \phi)} (e^{-i\tilde{\theta}_A} - e^{i\theta^+})(2 \cos \tilde{\theta}_A)^{-1}, \\ D' &= ue^{i(q^- - p^- - \phi)} (e^{-i\tilde{\theta}_A} - e^{i\theta^-})(2 \cos \tilde{\theta}_A)^{-1}. \end{aligned} \quad (21)$$

Here, we have defined

$$\begin{aligned} q^+ &= q^e \cos \theta^+ L, & q^- &= q^h \cos \theta^- L, \\ p^+ &= \tilde{p}^e \cos \tilde{\theta} L, & p^- &= \tilde{p}^h \cos \tilde{\theta}_A L. \end{aligned} \quad (22)$$

In the thin-barrier limit defined as $L \rightarrow 0$ and $U \rightarrow \infty$, one gets

$$\tilde{\theta} \rightarrow 0, \tilde{\theta}_A \rightarrow 0, q_{\pm} \rightarrow 0, p_{\pm} \rightarrow \mp \chi \quad (23)$$

with $\chi = LU/v_F$. This indicates that thermal conductance is π -periodic with respect to χ in this limit.

Finally, the normalized thermal conductance is given by

$$\kappa = \int_0^{\infty} \int_{-\pi/2}^{\pi/2} dE d\theta \cos \theta (1 - |r(E, \theta)|^2 - \text{Re}(\frac{\cos \theta_A}{\cos \theta}) |r_A(E, \theta)|^2) \frac{E^2}{\Delta_0 T^2 \cosh^2(\frac{E}{2T})} \quad (24)$$

with the gap at zero temperature $\Delta_0 \equiv \Delta(0)$.

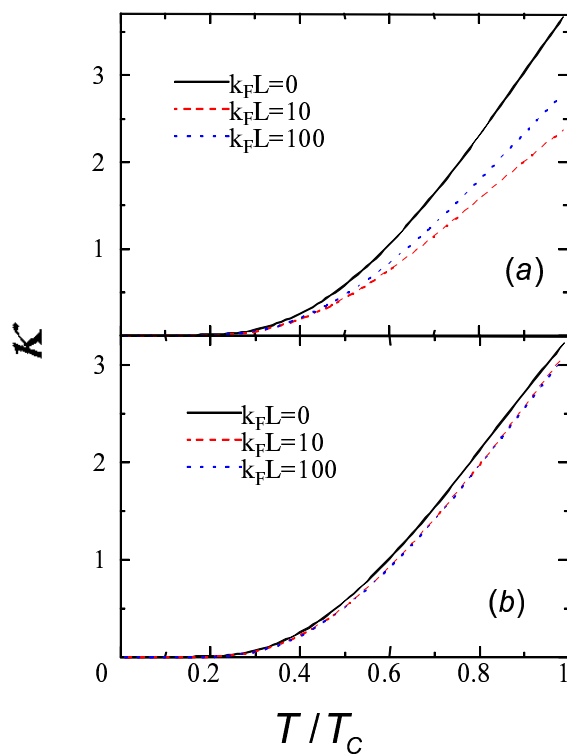


FIG. 2: (Color online) Thermal conductance as a function of T/T_C for various $k_F L$ with $U/E_F = 10$ and $E_F = E'_F = 100\Delta_0$ at $E_F = 100\Delta_0$ in (a) and $E_F = 10\Delta_0$ in (b).

We next present our results for the normalized thermal conductance. Figure 2 (a) shows thermal conductance as a function of T/T_C for various $k_F L$ with $U/E_F = 10$ and $E_F = E'_F = 100\Delta_0$. Here T_C is the transition temperature and $k_F \equiv E_F/v_F$. From Fig. 2 (a), an exponential dependence of the thermal conductance on temperature is seen, similar to the conventional normal metal/superconductor junctions.¹³ This exponential dependence reflects the s -wave

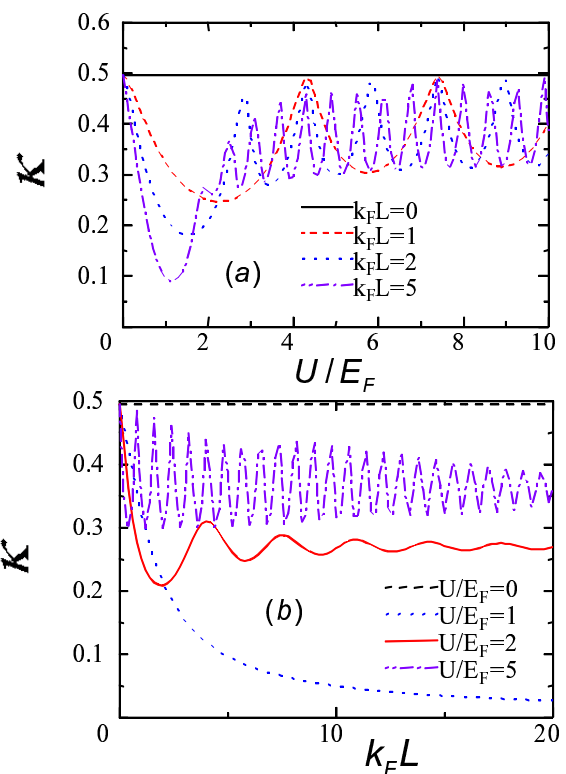


FIG. 3: (Color online) (a) Thermal conductance as a function of U/E_F for various $k_F L$ with $T/T_C = 0.5$ and $E_F = E'_F = 100\Delta_0$. (b) Thermal conductance as a function of $k_F L$ for various U/E_F with $T/T_C = 0.5$ and $E_F = E'_F = 100\Delta_0$.

symmetry of the superconductor. However, the length dependence of the thermal conductance is nonmonotonic (oscillatory) and thus essentially different from that in the conventional normal metal/superconductor junctions. A similar plot for $E_F = 10\Delta_0$ is shown in Fig. 2 (b). We also find an exponential temperature dependence, but the dependence on L gets weaker. Therefore, the magnitude of the oscillation with

respect to $k_F L$ gets reduced with the increase of the Fermi wave vector mismatch.

Figure 3 (a) depicts thermal conductance as a function of U/E_F for various length $k_F L$ with $T/T_C = 0.5$ and $E_F = E'_F = 100\Delta_0$. An oscillatory dependence of the thermal conductance on U/E_F is seen. The period decreases with $k_F L$. Figure 3 (b) displays thermal conductances as a function of $k_F L$ for various U/E_F with $T/T_C = 0.5$ and $E_F = E'_F = 100\Delta_0$. We also find an oscillatory dependence on $k_F L$. The period also decreases with U/E_F . These features stem from the π -periodicity of the thermal conductance with respect to $\chi = k_F L U/E_F$ in the limit of $U \gg E_F$ and $k_F L \ll 1$ similar to the junction conductance.^{16,17,24} In other words, the damped oscillatory behavior of the thermal conductance is a direct manifestation of the relativistic low-energy Dirac fermions. Also, the presence of the insulating region is essential for the oscillatory behavior.

Since we have assumed a homogeneous chemical potential in each of graphene regions, the experimental observation of the predicted effects require charge homogeneity of the graphene samples. This is a challenge, since electron-hole puddles in graphene imaged by a scanning single electron transistor device²⁵ suggest that such charge inhomogeneities play an important role in limiting the transport characteristics of graphene²⁶. In addition, we have neglected the spatial

variation of the superconducting gap near the interface. The suppression of the order parameter near the interface is expected to be least pronounced when the sharp edge criteria is satisfied and there is a large Fermi-vector mismatch. In the present case, this is precisely so, whence we do not expect our qualitative results to be affected by taking into account the reduction of the gap near the interface. Finally, we have assumed that there is no lattice mismatch at the interfaces and that these are smooth and impurity-free⁴. A more refined picture could be obtained by using more realistic models of the variation of the chemical potential, i.e. a continuous slope instead of a step-like variation.

In summary, we have studied heat transport in normal/superconducting graphene junctions. We found that the thermal conductance has an exponential dependence on temperature which reflects the s -wave symmetry of the superconductor but oscillatory dependence on the potential height or the length of the barrier region. This oscillatory dependence stems from the relativistic nature of fermions in graphene, essentially different from the result in the conventional normal metal/superconductor junctions.

T.Y. acknowledges support by the JSPS. J.L. and A.S. were supported by the Research Council of Norway, Grants No. 158518/431 and No. 158547/431 (NANOMAT), and Grant No. 167498/V30 (STORFORSK).

-
- ¹ T. Ando, J. Phys. Soc. Jpn. **74**, 777 (2005).
² M. I. Katsnelson and K. S. Novoselov, Solid State Commun. **143**, 3 (2007).
³ A. H. Castro Neto, F. Guinea, N. M. R. Peres, K. S. Novoselov and A. K. Geim, arXiv:0709.1163v1.
⁴ C. W. J. Beenakker, arXiv:0710.3848.
⁵ K. S. Novoselov, A. K. Geim, S. V. Morozov, D. Jiang, Y. Zhang, S. V. Dubonos, I. V. Grigorieva and A. A. Firsov, Science **306**, 666 (2004).
⁶ Y. Zhang, Y.-W. Tan, H. L. Stormer and P. Kim, Nature **438**, 201 (2005).
⁷ K. S. Novoselov, A. K. Geim, S. V. Morozov, D. Jiang, M. I. Katsnelson, I. V. Grigorieva, S. V. Dubonos, and A. A. Firsov, Nature **438**, 197 (2005).
⁸ K. S. Novoselov, E. McCann, S. V. Morozov, V. I. Fal'ko, M. I. Katsnelson, U. Zeitler, D. Jiang, F. Schedin, and A. K. Geim, Nat. Phys. **2**, 177 (2006).
⁹ K. Yang, Solid State Commun. **143**, 27 (2007).
¹⁰ H. B. Heersche, P. Jarillo-Herrero, J. B. Oostinga, L. M. K. Vandersypen and A. F. Morpurgo, Nature **446**, 56 (2007).
¹¹ J. Scott Bunch, Y. Yaish, M. Brink, K. Bolotin, and P. L. McEuen, Nano Lett. **5**, 287 (2005).
¹² C. Berger, Z. Song, X. Li, X. Wu, N. Brown, C. Naud, D. Mayou, T. Li, J. Hass, A. N. Marchenkov, E. H. Conrad, P. N. First, and W. A. de Heer, Science **312**, 1191 (2006).
¹³ A. F. Andreev, Sov. Phys. JETP **19**, 1228 (1964).
¹⁴ G. E. Blonder, M. Tinkham, and T. M. Klapwijk, Phys. Rev. B **25**, 4515 (1982).
¹⁵ C. W. J. Beenakker, Phys. Rev. Lett. **97**, 067007 (2006).
¹⁶ S. Bhattacharjee and K. Sengupta, Phys. Rev. Lett. **97**, 217001 (2006); S. Bhattacharjee, M. Maiti, and K. Sengupta, Phys. Rev. B **76**, 184514 (2007).
¹⁷ J. Linder and A. Sudbø, Phys. Rev. Lett. **99**, 147001 (2007); arXiv:0712.0831.
¹⁸ We underline that the notation "insulator" in this context refers to a normal segment of graphene in which one experimentally induces an effective potential barrier.
¹⁹ A. F. Morpurgo and F. Guinea, Phys. Rev. Lett. **97**, 196804 (2006).
²⁰ P. R. Wallace, Phys. Rev. **71**, 622 (1947).
²¹ K. Fossheim and A. Sudbø, *Superconductivity: Physics and applications*, John Wiley & Sons Ltd., Ch. 5 (2004).
²² A. K. Nguyen and A. Sudbø, Phys. Rev. B **60**, 15307 (1999); H. Kleinert, Phys. Rev. Lett., **84** 286 (2000).
²³ Note that these conditions are equivalent to $\hat{v}_x \psi|_{x=0} = \hat{v}_x \tilde{\psi}_I|_{x=0}$ and $\hat{v}_x \tilde{\psi}_I|_{x=L} = \hat{v}_x \Psi|_{x=L}$ with velocity operator $\hat{v}_x = \partial H / \partial k_x = v_F \sigma_x$ and hence the current is conserved at the interfaces.
²⁴ M. I. Katsnelson, K. S. Novoselov and A. K. Geim, Nature Phys. **2**, 620 (2006).
²⁵ J. Martin, N. Akerman, G. Ulbricht, T. Lohmann, J. H. Smet, K. von Klitzing and A. Yacoby, arXiv:0705.2180v1.
²⁶ E.-A. Kim and A. H. Castro Neto, arXiv:cond-mat/0702562v2.